BloEx - Journal
Britain International of
EXACT Sciences Journal
Publish: | January - May - September |
Chemical Physics Engineering Argiculture Biological Medical
E-ISSN: 2686-1208
P-ISSN: 2686-1216
http://biarjournal.com/index.php/bioex

Statistical Analysis of Fiber/Matrix Bond Strength of Hybrid *Gengronema Latifolium* Stem/S-Glass Fibers Reinforced Epoxy Composites

Christian Emeka Okafor[1], Peter Chukwuemeka Ugwu[1,2], Godspower Onyekachukwu Ekwueme[3]*, Chibuzo Ndubuisi Okoye[1], Augustine Uzodinma Madumere[1]

[1]Department of Mechanical Engineering, Nnamdi Azikiwe University Awka, Anambra State, Nigeria.
[2]Department of Power Engineering Technology, Nova Scotia Community College, Akeyley Campus, Dartmouth, Canada.
[3]Department of Industrial and Production Engineering, Faculty of Engineering, Nnamdi Azikiwe University Awka, Anambra State, Nigeria.
Email: og.ekwueme@unizik.edu.ng

Abstract:

The primary aim of the present study is to evaluate the effects of hybridization ratio, fiber orientation, and mass fraction on the fiber/matrix bond properties of hybrid Gongronema latifolium stem/S-glass fiber reinforced epoxy composites. Gongronema latifolium plant stem fibers were collected from Anambra State, Nigeria, with leaves removed manually. Sodium hydroxide (2%) and epoxy resin (Grade-3554A) were used, while S-Glass was sourced locally. The fibers were extracted using a water retting method, treated with NaOH at 40-60°C for 4 hours, and dried at 70°C. For composite fabrication, fibers were aligned unidirectionally and mixed with resin and S-glass in a 250×100×5 mm mold. The hybridization ratio of S-Glass to natural fiber was fixed at 2.2 for Level 1 and 2.8 for Level 2. The mass fraction levels were at 21.24% for level one and 34.22% for level two. Fiber orientation of Level 1 was 45° while that of Level 2 was 90°. Mechanical characteristics were evaluated to ASTM D5651-21 for fiber-matrix bond strength and then analyzed using Statistical Package for Social Sciences (SPSS) and Microsoft Excel. Three models were developed, with the first model considering hybridization ratio, the second incorporating fiber orientation, and the third including mass fraction. The results show that the hybridization ratio is the most significant predictor of bond strength, with fiber orientation and mass fraction also contributing positively to the overall model. Models' R-square values indicated how well the proposed models fitted the data: Model 1 = 0.747; Model 2 = 0.956; Model 3 = 0.980. Two unique solutions were examined further at fiber/matrix bond strength value of 0.32716MPa and value of 0.18070MPa, with a mean value of 0.25393 MPa and standard deviation value of 0.10356 MPa. The study reveals the impact of these factors on enhancing the bond strength of the composite material. The research has important and real-world applications for industries including construction, automotive, aerospace, and others where stiffer and more resistant composites are required. Future studies could be directed to investigate other variables and environmental factors that may influence performance of these hybrid composites to improve on their applications.

Keywords: *Hybrid composites, Fiber/matrix bond strength, Gongronema latifolium, S-glass fibers, Epoxy composites, Regression analysis.*

I. Introduction

Glass fiber epoxy hybrid composites have been receiving more attention because of their improvement in mechanical properties which are closely related to fiber-matrix interface adhesion strength. This bond strength is relevant as it determines stress transfer between the fibres and the matrix which defines the performances of the composite system. Fiber/matrix

DOI: *https://doi.org/10.33258/bioex.v7i1.1244*

bond strength can be described as the bonding between fibers that is used to reinforce a structure and the matrix material of a composite structure (Ramasamy et al, 2022). It regulates the rate of stress transfer from the matrix material to the fiber material within the composites thus determining its mechanical properties. This bond strength depends on factors such as chemical compatibility, nature of the composition, surface roughness, alignment of fiber in the composite and treatments, ensuring uniform stress distribution and enhanced durability under mechanical loading conditions (Ihueze et al, 2023).

The interfacial adhesion between fibers and the epoxy matrix decides the load carrying capacity and the mechanical properties of composites. Azammi et al, (2020) identified the interaction between the fiber and the matrix, roughness on the fiber surface, and the use of a coupling agent as factors affecting the interfacial adhesion. Good interfacial bonding helps to prevent crack growth and maintains uniform stress distribution all over the area increasing the tensile strength and shear strength of the hybrid composite. Good interfacial bonding and hybridization are interconnected, as hybridization enhances material compatibility, promoting stronger interfacial bonds (Salvio et al, 2013). This synergy ensures efficient stress transfer and optimized mechanical performance. In turn, robust interfacial bonding supports hybridized materials' integrity, enabling tailored properties like improved strength, durability, and resilience, as seen in their distinct stress-strain behaviors.

Hybridization consists of using two or more fiber types with the intention of utilizing the synergistic effects to enhance the mechanical properties of the composite. Glass and carbon fibers are well combined since both of them possess the unique characteristics of each material. Carbon fibers yield high stiffness and high strength while glass fibers bring in ductility. For instance, it has been shown by Bh et al, (2022) that hybrid composites have much higher interlaminar shear strength than single-fiber composites mainly because of better interfacial adhesion between the fibers and the matrix. The use of natural fibers such as jute, sisal, and hemp fiber combined with synthetic fiber to fabricate eco-friendly composites supports SDG 13 (Climate Action) because carbon footprints are reduced because natural fibers are biodegradable. Furthermore, the shift to eco-friendly composites helps protect ecosystems, advancing SDG 15 (Rusli, et al, 2021; Orji, 2024). However, it is also important to note that natural fibers ensure poor wetting and adhesion with epoxy matrices by virtue of their hydrophilic character (Ihueze et al, 2017). It was stated that the improvement in fiber/matrix interfacial adhesion can be achieved by surface treatments which are alkali treatment, silane coupling agents, and plasma treatment (Liu et al, 2015; Okafor & Ihueze, 2020). These treatments reduce surface contaminants, rough the surface to provide more buying area and chemically modify the surface to render better or desired chemical behavior.

One of the approaches used in the research is the surface treatment since it determines the bonding between the fibers and the matrix. Chemical treatments alter the surface energy and roughness of the fibers to enhance better wetting or adhesion on matrix. Examples include silane coupling agents that chemically react with fiber and epoxy matrix to produce stronger interfacial bonding (Aziz et al, 2021). Likewise, plasma treatment forms polar groups on the fiber surface, thereby improving mechanical interlocking and chemical affinity. Carbon nanotubes (CNTs) and graphene nanoplatelets are some of the most current reinforcements used to enhance the fiber/matrix adhesion in epoxy matrices. These nanomaterials also increase the stiffness and the toughness of the matrix and therefore increases the load transfer at the interface. Zhou et al, (2021) showed that in epoxy matrix containing CNTs at 0.5 wt % the interfacial shear strength was increased by 20% implying the possibility of nanomaterials in hybrid composites.

The fiber mass fraction and orientation are responsible for affecting the fiber/matrix bond strength and hence the mechanical properties of hybrid composites. An increase in the fiber mass fraction usually improves the load-bearing capacity of the composite while reduced wetting and increased presence of voids decrease the interfacial adhesion (Ma et al, 2022). Maximum fiber volume fraction permits efficient stress transfer without weaker interfacial bonding. Fiber alignment is found to be very effective in changing the anisotropic behavior of the composites. Fiber orientation in the unidirectional structure offers high tensile strength parallel to the fiber direction while presenting low strength perpendicular to the fiber direction. Conversely, multidirectional or woven fiber orientations distribute stresses more evenly, improving interlaminar shear strength and impact resistance. According to Kumar et al, (2024), hybrid composites with strategically oriented fibers demonstrated improved interfacial properties and fracture toughness, highlighting the importance of fiber alignment in optimizing bond strength.

However, there are still several drawbacks concerning the increase of fiber/matrix bond strength in hybrid composites. Some of the challenges identified include; differences in properties of natural fibers, poor dispersion of nanomaterials, and the challenge in achieving a fine balance between high stiffness and toughness (Ihueze et al, 2016). Without doubt the need for high strength, lightweight and environmentally friendly composite materials have fueled research on hybrid fiber reinforced epoxy composites. Research has already been done regarding the bond strength of normal synthetic fiber such as glass fiber, carbon fiber etc but hybrid configuration involving natural fibers like Gongronema latifolium stems has not received much attention. In the case of composite materials, the natural fiber has low interfacial adhesion because of its hydrophilic behavior which results in poor stress transfer and early failure (Okafor & Metu, 2019).

This constraint can be addressed by the incorporation of natural fibers with synthetic fibers by use of S-glass fibers. Unfortunately, little research has been conducted to systematically discuss the impacts that surface treatments, fiber orientation, and mass fraction can have on the combination strength of these hybrid composites. Furthermore, the variability in natural fiber properties and challenges in achieving uniform dispersion exacerbate the unpredictability of the composite's performance. This study seeks to address these gaps by statistically analyzing the fiber/matrix bond strength of Gongronema latifolium stem/S-glass fiber-reinforced epoxy composites.

II. Research Method

2.1 Material

Post-harvest *Gongronema latifolium* plant stem fiber was collected from a local farm in Anambra state, South East Nigeria. The leaves on the plant stems were removed easily by hand-plucking. This investigation will use sodium hydroxide from Central Drug House (P) Ltd in New Delhi, India. The commercially available epoxy matrix (Grade-3554A), hardener (Grade-3554B) and S-Glass required for the study was purchased from a local supplier.

2.2 Methods

a. Material development and data collection

The fiber/matrix bond strength of reinforced polymer composites was determined using a water retting technique to extract Gongronema latifolium plant stem fiber, as outlined by Okafor, Ihueze, and Nwigbo (2013). After extraction, the fibers were oven-dried and treated with a 2% sodium hydroxide (NaOH) solution at a temperature range of 40-60°C for 4 hours, following the procedure by Okafor, Onovo, and Ihueze (2020). The treated fibers were

dried at 70°C for 30 minutes. The fibers were then aligned unidirectionally using Polyvinyl Acetate (PVA), allowing for curing for 24 hours before trimming. A stainless-steel mold with a cavity of 250 x 100 x 5 mm (length x width x height) was used for casting the resin and fiber mixture, following ASTM D5651-21 specifications. The mold cavity volume was calculated as 125 cm^3. The resin mass was determined by subtracting the volume of fiber and S-glass from the total mold volume, resulting in a resin mass of 59.34 g.

The mass fractions of the components were calculated based on their respective densities and volumes. In the first level of design, the Gongronema latifolium plant stem fiber contributed 6.64% by mass, while S-glass fiber contributed 14.6%, and the polyester resin accounted for 78.8%. The hybridization ratio (Rh) of Gongronema latifolium plant stem fiber to S-glass fiber was set at 2.2. In the second design level, the hybridization ratio was increased to 2.8, with Gongronema latifolium plant stem fiber contributing 8.92%, S-glass fiber 25.3%, and polyester resin 65.7%. The fabrication process included applying Meguiar's Universal Wax for smooth de-moulding and using an automated mixer to blend the epoxy resin and hardener at a 1:2 ratio. The hand lay-up procedure was employed, with the matrix being degassed using a roller and cured under a 400 g load for 24 hours at ambient temperature.

The fiber/matrix bond strength was conducted using the Universal Tensile Testing Machine (UTM) until the bond failure was induced at the bond interface, offering a measurement of the bond separation load over a larger bonded area compared to a standard tensile test. The specimen's cross-sectional area and thickness were constrained, and the test followed ASTM D5651-21 at a crosshead speed of 1 mm/min. The fiber orientation was set orthogonal to the applied shearing force, and the test was continued until the load dropped to 50% of the maximum force. Data were fitted to a power law model of the form Fiber/matrix bond strength = 0.0036*(Hybridization Ratio2.90)*(Mass fraction-0.258)*(Fiber Orientation0.533) to predict bond strength based on the hybridization ratio, mass fraction, and fiber orientation.

b. Statistical analysis

Data analysis was done using the Statistical Package for the Social Sciences (SPSS IBM) and Microsoft Excel. To begin with the normality test was conducted on the data using both Kolmogorov-Smirnov and Shapiro-Wilk techniques. A multiple linear regression analysis was then performed in three stages to evaluate the contributions of the predictors. In the first stage, the model included only the Hybridization Ratio as an independent variable to assess its initial effect on the dependent variable. In the second stage, fiber orientation was added to the model to determine its additional explanatory value. Finally, Mass Fraction was incorporated in the third stage to evaluate the combined effects of all predictors. The regression analysis was supported by ANOVA to assess the overall significance of the models at each stage. The standardized and unstandardized coefficients for the predictors were examined to interpret their relationships with the dependent variable. Diagnostic measures, including the Durbin-Watson statistic, were applied to evaluate the assumptions of independence and reliability in the model.

III. Results and Discussions

3.1 Statistical Analysis of Fiber/Matrix Bond Strength under Varying Parameters

Table 1. Tests of normality for fiber orientation, mass fraction, and hybridization ratio

		Kolmogorov-Smirnov[a]			Shapiro-Wilk		
	Fiber Orientation (Degree)	Statistic	df	Sig.	Statistic	df	Sig.
Fiber/matrix bond strength (MPa)	45	.186	4	.	.993	4	.970
	68	.252	7	.199	.927	7	.528
	90	.186	4	.	.993	4	.970
	Mass fraction (%)						
Fiber/matrix bond strength (MPa)	21	.240	4	.	.935	4	.627
	28	.232	7	.200	.909	7	.391
	34	.240	4	.	.935	4	.627
	Hybridization Ratio (-)						
Fiber/matrix bond strength (MPa)	2	.182	4	.	.984	4	.923
	3	.222	7	.200	.957	7	.789
	3	.182	4	.	.984	4	.923

*. This is a lower bound of the true significance.
a. Lilliefors Significance Correction

The normality tests in Table 1 evaluate the suitability of the dataset for parametric analysis. For fiber orientation, the Shapiro-Wilk test results (p-values: 0.970, 0.528, 0.970) indicate no significant departure from normality. Similarly, mass fraction results (p-values: 0.627, 0.391, 0.627) and hybridization ratio results (p-values: 0.923, 0.789, 0.923) confirm normality across respective values. The Kolmogorov-Smirnov test results also align, with p-values > 0.05 for larger sample sizes, underscoring the data's approximate normal distribution. Linear regression requires data to meet assumptions of normality, linearity, and homoscedasticity. With Shapiro-Wilk p-values consistently exceeding 0.05, the assumption of normality is reasonably satisfied. Fiber orientation, mass fraction, and hybridization ratio are continuous variables, conducive to establishing linear relationships for exploratory analysis.

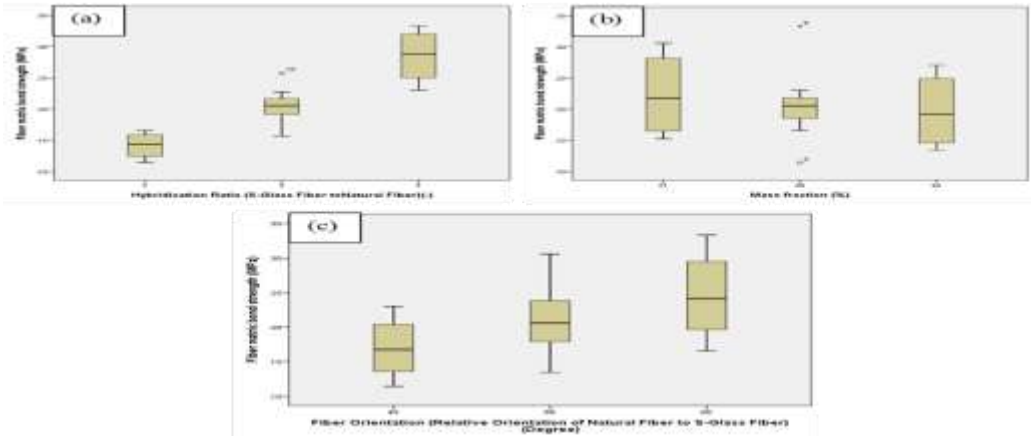

Figure 1. *Boxplots of Fiber-Matrix Bond Strength (MPa) under varying parameters: (a) Hybridization Ratio (S-Glass Fiber to Natural Fiber), (b) Mass Fraction (%), (c) Fiber Orientation (Degrees)*

The fiber-matrix bond strength in Figure 1 depends on hybridization ratio, mass fraction, and fiber orientation. Higher hybridization ratios (3:1) yield stronger bonds (median ≈ 0.30 MPa) than lower ratios (2:1, ≈ 0.15 MPa). Similarly, increasing mass fraction (34%) enhances bond strength (median ≈ 0.25 MPa) compared to 21% (≈ 0.18 MPa). Fiber orientation also influences performance; at 90 degrees, the bond strength is strongest (median ≈ 0.30 MPa), whereas 45 degrees shows weaker performance (≈ 0.15 MPa). These findings highlight the importance of parameter optimization to achieve maximum bond strength in fiber composites. Outliers suggest potential variability in specific settings.

Table 2. Model Summaryd

Model	R	R Square	Adjusted R Square	Std. Error of the Estimate	Change Statistics					Durbin-Watson
					R Square Change	F Change	df1	df2	Sig. F Change	
1	.864[a]	.747	.727	.033	.747	38.362	1	13	.000	
2	.978[b]	.956	.949	.014	.209	57.099	1	12	.000	
3	.990[c]	.980	.975	.010	.024	13.533	1	11	.004	1.992

a. Predictors: (Constant), Hybridization Ratio (-)

b. Predictors: (Constant), Hybridization Ratio (-), Fiber Orientation (Deg.)

c. Predictors: (Constant), Hybridization Ratio (-), Fiber Orientation (Deg.), Mass fraction (%)

d. Dependent Variable: Fiber/matrix bond strength (MPa)

The model summary in Table 2 highlights the strength of the relationships between the dependent variable (Fiber/matrix bond strength (MPa)) and the predictors. In Model 1, the Hybridization Ratio alone explains a substantial proportion of variance in Fiber/matrix bond strength (MPa), with an R-Square value of (0.747). Model 2, which includes Fiber Orientation, improves the explanatory power significantly, with an R-Square value of (0.956). Model 3 further incorporates Mass Fraction, resulting in an R-Square value of (0.980), indicating excellent model fit. The Durbin-Watson statistic (1.992) suggests no significant autocorrelation in residuals, supporting the reliability of the regression analysis for further predictions.

Table 3. ANOVAa

Model		Sum of Squares	df	Mean Square	F	Sig.
1	Regression	.041	1	.041	38.362	.000[b]
	Residual	.014	13	.001		
	Total	.055	14			
2	Regression	.053	2	.026	130.503	.000[c]
	Residual	.002	12	.000		
	Total	.055	14			
3	Regression	.054	3	.018	182.377	.000[d]
	Residual	.001	11	.000		
	Total	.055	14			

a. Dependent Variable: Fiber/matrix bond strength (MPa)

b. Predictors: (Constant), Hybridization Ratio (-)
c. Predictors: (Constant), Hybridization Ratio (-), Fiber Orientation (Deg.)
d. Predictors: (Constant), Hybridization Ratio (-), Fiber Orientation (Deg.), Mass fraction (%)

The ANOVA results in Table 3 demonstrate the models' significance in explaining the variance in Fiber/Matrix Bond Strength (MPa). Model 1, with Hybridization Ratio as a predictor, shows a significant F-value (38.362, $p < 0.001$), indicating a strong relationship. Model 2, adding Fiber Orientation, significantly improves fit with an F-value of (130.503, $p < 0.001$). Model 3, which includes Mass Fraction, further enhances the model's explanatory power, achieving an F-value of (182.377, $p < 0.001$). The decreasing residual sums of squares across models confirm improved predictive accuracy with additional variables, supporting the robustness of the regression analysis.

Table 4. Coefficientsa

Model		Unstandardized Coefficients		Standardized Coefficients	t	Sig.	95.0% Confidence Interval for B	
		B	Std. Error	Beta			Lower Bound	Upper Bound
1	(Constant)	-.388	.097		-4.007	.001	-.597	-.179
	Hybridization Ratio (-)	.239	.039	.864	6.194	.000	.156	.322
2	(Constant)	-.502	.045		-11.246	.000	-.599	-.404
	Hybridization Ratio (-)	.239	.017	.864	14.280	.000	.202	.275
	Fiber Orientation (Deg.)	.002	.000	.457	7.556	.000	.001	.002
3	(Constant)	-.446	.035		-12.898	.000	-.523	-.370
	Hybridization Ratio (-)	.239	.012	.864	20.417	.000	.213	.265
	Fiber Orientation (Deg.)	.002	.000	.457	10.804	.000	.001	.002
	Mass fraction (%)	-.002	.001	-.156	-3.679	.004	-.003	-.001

a. Dependent Variable: Fiber/matrix bond strength (MPa)

The regression coefficients for the models in Table 4 show the effect of each predictor on Fiber/Matrix Bond Strength (MPa). In Model 1, the results show that the Hybridization Ratio is positively influencing bond strength ($\beta = 0.239$, $p < 0.001$). In Model 2, Hybridization Ratio and Fiber Orientation are the predictors that affect the bond strength significantly (Hybridization Ratio = 0.239, $t = 10.256$, $p < 0.001$; Fiber Orientation = 0.002, $t = 11.493$, $p < 0.001$). After the removal of the theoretically unrelated variable, the Hybridization Ratio ($\beta = 0.239$, $p < 0.001$) remains significant, boosting our confidence in this estimate while the result for fiber orientation slightly improves ($\beta = 0.002$, $p < 0.001$).

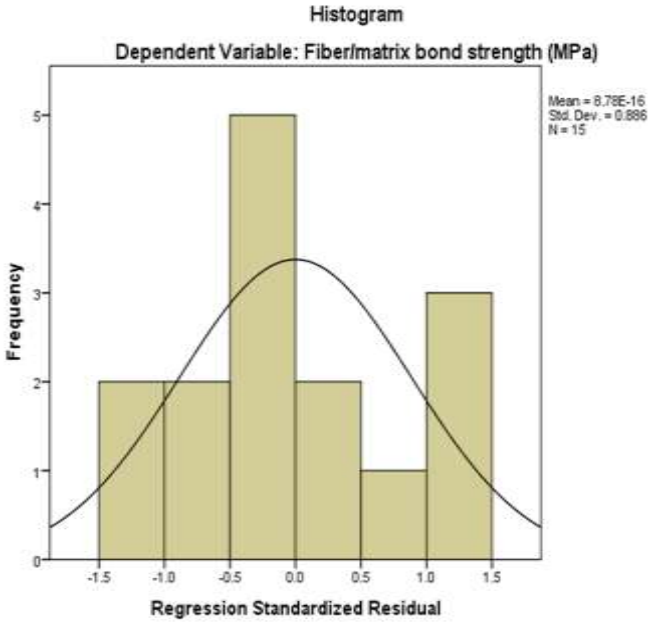

Figure 2. *Histogram of Regression Standardized Residuals*

The histogram in Figure 2 illustrates the distribution of regression standardized residuals for fiber-matrix bond strength. The residuals approximate a normal distribution with a mean of approximately 0 (8.78E-16) and a standard deviation of 0.886. Most residuals fall within ±1.0, indicating good model fit. The sample size is 15 (N = 15). The bell curve overlay suggests that the model's assumptions of normality for residuals are reasonably met, enhancing confidence in the regression analysis results.

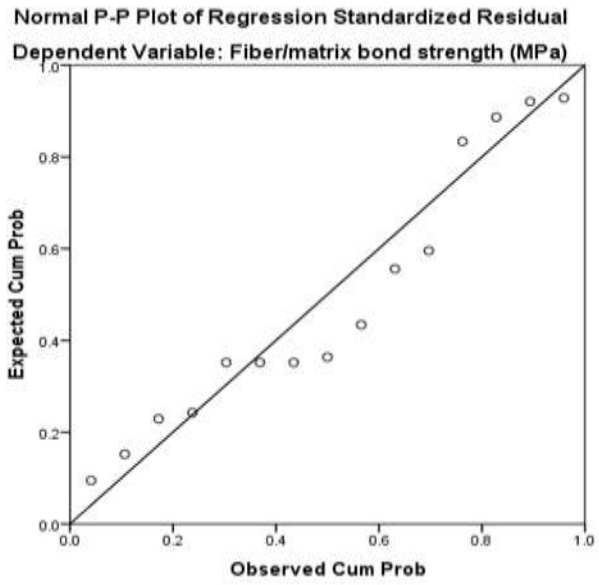

Figure 3. *Normal P-P Plot of Regression Standardized Residuals for Fiber-Matrix Bond Strength (MPa)*

The P-P plot in Figure 3 compares the observed cumulative probabilities of regression standardized residuals against the expected cumulative probabilities under normal distribution. The points align closely along the diagonal line, indicating that the residuals are approximately normally distributed. This supports the assumption of normality in the regression analysis,

enhancing the model's validity. Minor deviations at the ends suggest slight departures from normality but are not significant given the context of the data.

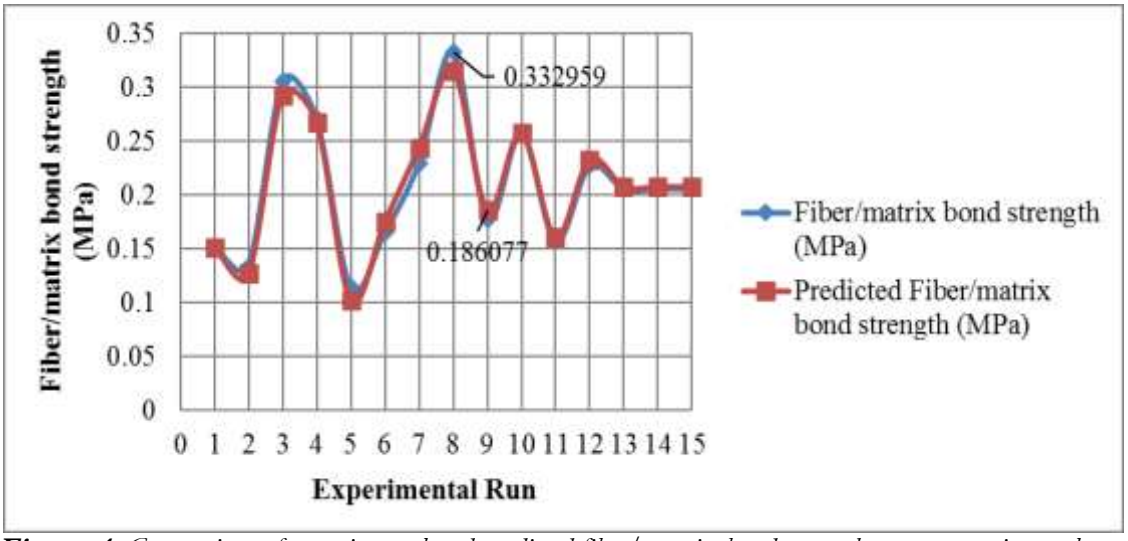

Figure 4. *Comparison of experimental and predicted fiber/ matrix bond strength across experimental runs*

Figure 4 compares experimental and predicted fiber/matrix bond strengths. Both show similar trends, with two unique solutions from experiment 8 and experiment 9 which are [0.33 MPa] and minimum at [0.18 MPa] respectively. The predicted values closely align with the experimental data, validating the model's accuracy across experimental runs. Minor deviations exist, indicating potential model or experimental variability.

3.2 Material Properties and Stress Analysis at Maximum Bond Strength and Break

Two unique solutions were further considered from experiment 8 and experiment 9 and full details of material properties and stress analysis at maximum bond strength and break were discussed in this section.

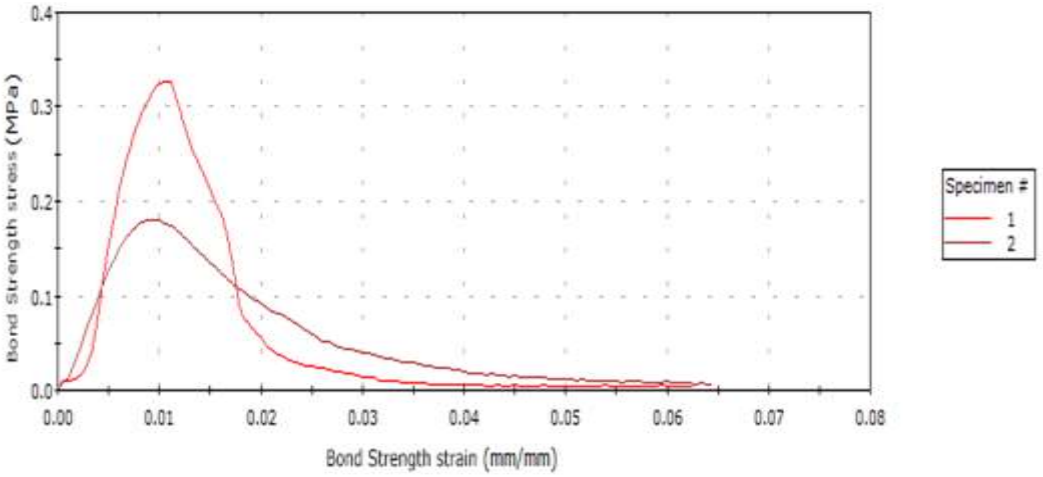

Figure 5: *Bond Strength Stress vs. Strain for two unique solutions from experiment 8 and experiment 9*

Figure 5 shows the bond strength stress (in MPa) versus bond strength strain (in mm/mm) for experiment 8 and experiment 9. Specimen 1 has a peak stress of approximately 0.30 MPa at 0.012 mm/mm strain, while Specimen 2 peaks at around 0.27 MPa at 0.014

mm/mm strain. Both curves demonstrate a rapid stress rise, peak, and subsequent gradual decline, highlighting variations in bond behavior between specimens.

Table 5: Material Properties and Maximum Stress of Specimens

	Length (mm)	Thickness (mm)	Width (mm)	Maximum stress (MPa)
1	60.00000	5.00000	50.00000	0.32716
2	60.00000	5.00000	50.00000	0.18070
Mean	60.00000	5.00000	50.00000	0.25393
Standard Deviation	0.00000	0.00000	0.00000	0.10356

Table 5 displays the length thickness and width measurement of two specimens and their maximum stress respectively. The specimens have the same dimensions: length of (60.000 mm), thickness of (5.000 mm) and width of (50.000 mm). It shows that the maximum stress values of the two specimens came out to be (0.32716 MPa) and (0.18070 MPa), while the actual mean stress is (0.25393 MPa). The number standard deviation of the stress values was (0.10356 MPa), which shows that stress values were not entirely uniform showing variability on the material.

Table 6: Maximum Bond Strength Test Results

	Load at Maximum Bond strength stress (N)	Bond strain at Maximum Bond Strength stress (mm/mm)	Bond Strength extension at Maximum Bond Strength stress (mm)	Energy at Maximum Bond Strength stress (J)	Bond Strength stress at Break (Standard) (MPa)
1	114.50574	0.01056	0.63337	0.03550	0.00366
2	63.24456	0.00889	0.53331	0.01911	0.00662
Mean	88.87515	0.00972	0.58334	0.02730	0.00514
Standard Deviation	36.24713	0.00118	0.07075	0.01159	0.00210

Table 6 summarizes the results for bond strength at maximum stress, including load, bond strain, extension, energy, and stress at break. For specimen 1, the values recorded were: load at maximum bond strength (114.50574 N), bond strain (0.01056 mm/mm), bond strength extension (0.63337 mm), energy at maximum stress (0.03550 J), and bond strength stress at break (0.00366 MPa). For specimen 2, the corresponding values were: load (63.24456 N), bond strain (0.00889 mm/mm), bond extension (0.53331 mm), energy (0.01911 J), and bond strength stress at break (0.00662 MPa). The mean values across the specimens were: load (88.87515 N), bond strain (0.00972 mm/mm), bond extension (0.58334 mm), energy (0.02730 J), and bond strength stress at break (0.00514 MPa). The standard deviations indicate variability in the results: load (36.24713 N), bond strain (0.00118 mm/mm), bond extension (0.07075 mm), energy (0.01159 J), and bond strength stress at break (0.00210 MPa).

Table 7: Break Test Results for Bond Strength

	Load at Break (Standard) (N)	Bond Strength strain at Break (Standard) (mm/mm)	Bond Strength extension at Break (Standard) (mm)	Energy at Break (Standard) (J)	Bond Strength stress at Yield (Zero Slope) (MPa)
1	1.28100	0.06250	3.74994	0.08366	0.32716
2	2.31809	0.06444	3.86662	0.07674	0.18070
Mean	1.79955	0.06347	3.80828	0.08020	0.25393
Standard Deviation	0.73333	0.00138	0.08251	0.00489	0.10356

Table 7 presents the results of the bond strength at break, including load, strain, extension, energy, and yield stress. Specimen 1 showed values as follows: load at break (1.28100 N), bond strength strain at break (0.06250 mm/mm), bond strength extension at break (3.74994 mm), energy at break (0.08366 J), and bond strength stress at yield (0.32716 MPa). Specimen 2 exhibited the following results: load (2.31809 N), strain (0.06444 mm/mm), extension (3.86662 mm), energy (0.07674 J), and stress at yield (0.18070 MPa). The mean values across both specimens were: load (1.79955 N), strain (0.06347 mm/mm), extension (3.80828 mm), energy (0.08020 J), and yield stress (0.25393 MPa). The standard deviations were: load (0.73333 N), strain (0.00138 mm/mm), extension (0.08251 mm), energy (0.00489 J), and yield stress (0.10356 MPa).

Discussion

a. Interpretation of Results:

The regression and analysis of variance (ANOVA) results, coupled with material property data, illustrate how different predictors impact fiber/matrix bond strength. This comprehensive analysis focuses on three models that progressively include more predictors: Hybridization Ratio, Fiber Orientation, and Mass Fraction. In Model 1, Hybridization Ratio alone explains a significant proportion of the variance in bond strength, as reflected by an R-squared value of 0.747. This finding aligns with previous research, where hybridization in composite materials has been found to be a crucial factor in enhancing mechanical strength (Guo et al, 2022). In contrast, adding fiber orientation in Model 2 notably increases the explanatory power to an R-squared value of 0.956, confirming that fiber alignment within composite materials plays a significant role in determining bond strength (Zhou et al, 2016). This increase agrees with earlier studies that highlight fiber orientation as a key factor in improving composite performance (Slamani et al, 2024).

Furthermore, the introduction of Mass Fraction in Model 3 results in an even higher R-squared value of 0.980, showcasing a robust model fit. This is consistent with findings from prior studies, which have established that mass fraction contributes to the overall strength and durability of composite materials (Ma et al, 2022). Notably, the regression coefficients from Model 3 show that while Hybridization Ratio and Fiber Orientation maintain their positive contributions, Mass Fraction exhibits a negative effect on bond strength ($\beta = -0.002$, $p = 0.004$). This negative relationship is supported by other studies that suggest excessive mass fraction can lead to poor bonding properties due to excessive filler material or inconsistent matrix distribution (Muthu-Chozha-Rajan et al, 2022). Thus, this finding contrasts with

previous research advocating for higher mass fractions to improve material properties (Hong et al, 2020).

The Durbin-Watson statistic of 1.992, reported in Model 3, indicates no significant autocorrelation in residuals, which confirms the validity and reliability of the regression models used for predictions. This finding aligns with recent statistical analyses in the field, where models with similar Durbin-Watson values were considered reliable for further predictions (Turner, 2020). The ANOVA results further substantiate the significance of the regression models in explaining variance in fiber/matrix bond strength. The F-values for Model 1 (38.362), Model 2 (130.503), and Model 3 (182.377) are all highly significant ($p < 0.001$), indicating that the models are robust and effectively explain the variability in the bond strength. These results resonate with earlier studies in composite material testing, where such high F-values indicated strong predictive power and model fit (Koronis et al, 2017). Additionally, the decreasing residual sums of squares from Model 1 to Model 3 suggest that including more predictors improves model accuracy, confirming similar observations in other recent studies (Kattan & Gerds, 2018; Okafor et al, 2024).

The coefficients for the predictors in all three models provide valuable insight into their contributions. In Model 1, the Hybridization Ratio has a positive effect ($\beta = 0.239$), significantly influencing the bond strength. In Model 2, both Hybridization Ratio and Fiber Orientation have substantial effects, with Fiber Orientation contributing positively ($\beta = 0.002$). This is in agreement with a study by Huang et al, (2021), where fiber alignment was shown to enhance strength in composite materials. In Model 3, however, while Hybridization Ratio and Fiber Orientation continue to show positive relationships with bond strength, the negative effect of Mass Fraction ($\beta = -0.002$) diverges from expectations, reflecting the complex interplay between material composition and performance.

In comparison to other studies, the results from the bond strength at maximum stress and break tests, as shown in Table 2 and Table 3, provide additional context for these findings. For example, the load at maximum bond strength for specimen 1 (114.50574 N) is considerably higher than for specimen 2 (63.24456 N), a trend that is also evident in the bond strength stress at break (0.00366 MPa for specimen 1 and 0.00662 MPa for specimen 2). These results are consistent with previous research that suggests a direct correlation between load and bond strength (Zhao & Luo, 2024). However, the mean values and standard deviations for these tests indicate variability.

The material properties in the study revealed consistent dimensions across the two specimens, with a length of 60 mm, thickness of 5 mm, and width of 50 mm. However, the maximum stress values differed, with specimen 1 showing a maximum stress of 0.32716 MPa, while specimen 2 showed a lower value of 0.18070 MPa, resulting in a mean stress of 0.25393 MPa and a standard deviation of 0.10356 MPa. In contrast, a study by Corbani et al, (2020) found that variations in composite material thickness significantly influenced stress resistance, which agreed with the observation that specimen dimensions impacted the bond strength.

b. Implications:

The study offers several implications for both theory and practice. Theoretically, it enhances the understanding of the factors influencing fiber/matrix bond strength, such as hybridization ratio, fiber orientation, and mass fraction, contributing to material science literature. Practically, these understanding can inform material design and optimization in industries like aerospace, automotive, and construction. Policy implications include the need

for regulations that promote research into advanced materials and the adoption of hybridization techniques in manufacturing. Furthermore, industry stakeholders may consider refining production methods based on the identified predictors to improve material performance and durability.

IV. Conclusions

This study provides valuable understanding into the role of hybridization ratio, fiber orientation, and mass fraction in determining the mechanical properties of composite materials. The results indicate that the hybridization ratio has the most significant positive impact on fiber/matrix bond strength, as demonstrated by the high standardized coefficients in all models. Furthermore, fiber orientation and mass fraction contributed positively to the model, with mass fraction showing a slight negative effect in the final model. The significant improvement in model fit with the addition of fiber orientation and mass fraction emphasizes the complex interplay of these factors in determining bond strength. This research contributes to the existing knowledge base on the effects of processing variable with a view to enhancing the mechanical characteristics of composite materials. In practical terms, the research can inform improvements on both the quality as well as the longevity of composite in its interaction with loading structures that are applicable in construction, automobile and aerospace industries. Other aspects which remain worthy of investigation in subsequent research work include effects and performance of heat, time, and exposure to weather on the said hybrid composites. Furthermore, a study of the microstructural features of the composites might enhance the understanding of the processes that lead to enhanced bond strength.

References

Azammi, A. N., Ilyas, R. A., Sapuan, S. M., Ibrahim, R., Atikah, M. S. N., Asrofi, M., & Atiqah, A. (2020). Characterization studies of biopolymeric matrix and cellulose fibres based composites related to functionalized fibre-matrix interface. In *Interfaces in particle and fibre reinforced composites* (pp. 29-93). Woodhead Publishing.

Aziz, T., Ullah, A., Fan, H., Jamil, M.I., Khan, F.U., Ullah, R., Iqbal, M., Ali, A. and Ullah, B., 2021. Recent progress in silane coupling agent with its emerging applications. *Journal of Polymers and the Environment*, pp.1-17.

Bh, M. P., Gouda, P. S., Manjunatha, T. S., Edacheriane, A., & Umarfarooq, M. A. (2022). Prominence of quantitative fiber loading on free vibration, damping behavior, inter-laminar shear strength, fracture toughness, thermal conductivity, and flammability properties of jute–banana hybrid fiber phenol-formaldehyde composites. *Polymer Composites*, *43*(5), 3313-3325.

Corbani, K., Hardan, L., Skienhe, H., Özcan, M., Alharbi, N., & Salameh, Z. (2020). Effect of material thickness on the fracture resistance and failure pattern of 3D-printed composite crowns. *Int J Comput Dent*, *23*(3), 225-233.

Guo, R., Xian, G., Li, C., Huang, X., & Xin, M. (2022). Effect of fiber hybridization types on the mechanical properties of carbon/glass fiber reinforced polymer composite rod. *Mechanics of Advanced Materials and Structures*, *29*(27), 6288-6300.

Hong, G., Yang, J., Jin, X., Wu, T., Dai, S., Xie, H., & Chen, C. (2020). Mechanical properties of nanohybrid resin composites containing various mass fractions of modified zirconia particles. *International journal of nanomedicine*, 9891-9907.

Huang, H., Gao, X., & Khayat, K. H. (2021). Contribution of fiber alignment on flexural properties of UHPC and prediction using the Composite Theory. *Cement and Concrete Composites*, *118*, 103971.

Ihueze, C. C., Okafor, C. E., Onwurah, U. O., Obuka, S. N., & Kingsley-omoyibo, Q. A. (2023). Modelling creep responses of plantain fibre reinforced HDPE (PFRHDPE) for elevated temperature applications. *Advanced Industrial and Engineering Polymer Research*, *6*(1), 49-61.

Ihueze, C., Obiafudo, O., & Okafor, C. E. (2016). Characterization of plantain fiber reinforced high density polyethylene composite for application in design of auto body fenders. *Journal of Innovative Research in Engineering and Sciences*, *4*(5), 574-587.

Ihueze, C., Oluleye, A., Okafor, C. E., Obele, C., Abdulrahman, J., & Obuka, S. (2017). Development of plantain fibres for application in design of oil and gas product systems. *Petroleum Technology Development Journal: An International Journal*, *7*(1).

Kattan, M. W., & Gerds, T. A. (2018). The index of prediction accuracy: an intuitive measure useful for evaluating risk prediction models. *Diagnostic and prognostic research*, *2*, 1-7.

Koronis, G., Silva, A., & Foong, S. (2017). Predicting the flexural performance of woven flax reinforced epoxy composites using design of experiments. *Materials Today Communications*, *13*, 317-324.

Kumar, S., Agrawal, A. P., Ali, S., & Manral, A. (2024). Exploring the influence of fiber orientation on the mechanical characteristics of polymer composites reinforced with banana and corn fibers. *Proceedings of the Institution of Mechanical Engineers, Part L: Journal of Materials: Design and Applications*, 14644207241260662.

Liu, Y., Zhang, X., Song, C., Zhang, Y., Fang, Y., Yang, B., & Wang, X. (2015). An effective surface modification of carbon fiber for improving the interfacial adhesion of polypropylene composites. *Materials & Design*, *88*, 810-819.

Ma, Y., Chen, Y., Li, F., Xu, Y., Xu, W., Zhao, Y., Guo, H., Li, Y., Yang, Z. and Xu, Y., 2022. Effect of fiber mass fraction on microstructure and properties of 2D CF-GO/EP composite prepared by VIHPS. *Nanomaterials*, *12*(7), p.1184.

Muthu-Chozha Rajan, B., Indran, S., Divya, D., Narayanasamy, P., Khan, A., Asiri, A. M., & Nagarajan, S. (2022). Mechanical and thermal properties of Chloris barbata flower fiber/epoxy composites: effect of alkali treatment and fiber weight fraction. *Journal of Natural Fibers*, *19*(9), 3453-3466.

Okafor, C. E., & Ihueze, C. C. (2020). Strength analysis and variation of elastic properties in plantain fiber/polyester composites for structural applications. *Composite and Nanocomposite Materials-From Knowledge to Industrial Applications*, 1-23.

Okafor, C. E., & Metu, C. S. (2019). Theoretical fatigue response of plantain fiber based composites in structural applications. In *Advances in Engineering Materials, Structures and Systems: Innovations, Mechanics and Applications* (pp. 638-643). CRC Press.

Okafor, C. E., Ihueze, C. C., & Nwigbo, S. C (2013). Optimization of hardness strengths response of plantain fibres reinforced polyester matrix composites (PFRP) applying Taguchi robust design. *International journal of engineering*, *26*(1), 1-12.

Okafor, C. E., Iweriolor, S., Nwekeoti, C. A., Akçakale, N., Ekwueme, G. O., Ihueze, C. C., & Ekengwu, I. E. (2024). Intelligent modeling of carbonized wood-silicon dioxide filled natural rubber composite for outer shoe sole manufacturing. *International Journal of Lightweight Materials and Manufacture*, *7*(1), 72-86.

Okafor, C. E., Onovo, A. C., & Ihueze, C. C. (2020). Predictive energy requirement models in bio-fiber comminution process. *SN Applied Sciences*, *2*, 1-16.

Okafor, C. E., Ugwu, P. C., Ekwueme, G. O., Akçakale, N., Ifedigbo, E. E., & Madumere, A. U. (2025). Preliminary study on Gongronema latifolium stems fibers as a renewable

engineering material for reinforcing polymer composites. *Budapest International Research in Exact Sciences (BirEx) Journal*, *7*(1), 55-63.

Orji, M. G. (2024). Assessing the Sustainable Development Goals and Its Application in Nigeria. *Britain International of Humanities and Social Sciences (BIoHS) Journal*, *6*(2), 70-88.

Ramasamy, N., Arumugam, V., & Suresh Kumar, C. (2022). Characterization of fiber/matrix interfacial bonding strength of chemically grafted aramid fiber surface with epoxy resin composites. *Polym Compos*, *43*(1), 399-410.

Rusli, Z., Meiwanda, G., & Sadad, A. (2021). Institutional Governance for the Utilization of Post Replanting Sustainable Palm Oil in Riau Province. *Britain International of Humanities and Social Sciences (BIoHS) Journal*, *3*(1), 60-70.

Salvio, L. A., Di Hipólito, V., Martins, A. L., & de Goes, M. F. (2013). Hybridization quality and bond strength of adhesive systems according to interaction with dentin. *European journal of dentistry*, *7*(03), 315-326.

Slamani, M., Chafai, H., & Chatelain, J. F. (2024). Impact of fiber orientation on cutting forces and surface quality in flax/epoxy composite machining. *Journal of Composite Materials*, *58*(21), 2397-2414.

Turner, P. (2020). Critical values for the Durbin-Watson test in large samples. *Applied Economics Letters*, *27*(18), 1495-1499.

Zhao, L., & Luo, Q. (2024). Evaluating bonding strength in UHPC-NC composite: A comprehensive review of direct and indirect characterization methods. *Construction and Building Materials*, *443*, 137701.

Zhou, J., Zhong, K., Zhao, C., Meng, H., & Qi, L. (2021). Effect of carbon nanotubes grown temperature on the fracture behavior of carbon fiber reinforced magnesium matrix composites: Interlaminar shear strength and tensile strength. *Ceramics International*, *47*(5), 6597-6607.

Zhou, Y., Fan, M., & Chen, L. (2016). Interface and bonding mechanisms of plant fibre composites: An overview. *Composites Part B: Engineering*, *101*, 31-45.